Applied Thermal Engineering 86 (2015) 199–213

Contents lists available at ScienceDirect

Applied Thermal Engineering

journal homepage: www.elsevier.com/locate/apthermeng

Research paper

# Energy and geotechnical behaviour of energy piles for different design solutions

Niccolò Batini [a], Alessandro F. Rotta Loria [a, *], Paolo Conti [b], Daniele Testi [b], Walter Grassi [b], Lyesse Laloui [a]

[a] Swiss Federal Institute of Technology in Lausanne, EPFL, Laboratory of Soil Mechanics, EPFL-ENAC-IIC-LMS, Station 18, 1015 Lausanne, Switzerland
[b] University of Pisa, Department of Energy, Systems, Territory and Constructions Engineering, DESTEC, Building Energy Technique and TEchnology Research Group, BETTER, Largo Lucio Lazzarino, 56122 Pisa, Italy

## HIGHLIGHTS

- Energy piles thermo-mechanical behaviour crucially depends on pipes configuration.
- Thermal power extracted from the ground increases with pile aspect ratio.
- Heat transfer rate fundamentally depends on fluid mass flow rate.
- Heat transfer rate is not markedly affected by operative antifreeze concentrations.

## ARTICLE INFO

*Article history:*
Received 26 January 2015
Accepted 21 April 2015
Available online 30 April 2015

*Keywords:*
Energy piles
Thermo-mechanical behaviour
Energy performance
Geotechnical performance
Design configurations

## ABSTRACT

Energy piles are heat capacity systems that have been increasingly exploited to provide both supplies of energy and structural support to civil structures. The energy and geotechnical behaviours of such foundations, which are governed by their response to thermo-mechanical loads, is currently not fully understood, especially considering the different design solutions for ground-coupled heat exchangers. This paper summarises the results of numerical sensitivity analyses that were performed to investigate the thermo-mechanical response of a full-scale energy pile for different *(i)* pipe configurations, *(ii)* foundation aspect ratios, *(iii)* mass flow rates of the fluid circulating in the pipes and *(iv)* fluid mixture compositions. This study outlines the impacts of the different solutions on the energy and geotechnical behaviour of the energy piles along with important forethoughts that engineers might consider in the design of such foundations. It was observed that the pipe configuration strongly influenced both the energy and the geotechnical performance of the energy piles. The foundation aspect ratio also played an important role in this context. The mass flow rate of the fluid circulating in the pipes remarkably influenced only the energy performance of the foundation. Usual mixtures of a water-antifreeze liquid circulating in the pipes did not markedly affect both the energy and the geotechnical performance of the pile.



## 1. Introduction

Energy piles (EP) are a relatively new technology that couples the structural role of canonical pile foundations to that of heat exchangers. These foundations, already needed to provide structural support to the superstructure, are equipped with pipes with a heat carrier fluid circulating into them to exploit the large thermal storage capabilities of the ground for the heating and cooling of buildings and infrastructures, particularly when these EPs are coupled to heat pumps. In these systems, heat is exchanged between the foundations and the soil in a favourable way, as the undisturbed temperature of the ground at a few metres of depth remains relatively constant throughout the year (being warmer than the ambient temperature in the winter and cooler in the summer) and the thermal storage capacities of both media are advantageous for withstanding the process. Geothermal heat pumps are connected to the piles and can transfer the stored heat and their energy input to buildings and infrastructures during the

* Corresponding author.
*E-mail address:* alessandro.rottaloria@epfl.ch (A.F. Rotta Loria).

http://dx.doi.org/10.1016/j.applthermaleng.2015.04.050
1359-4311/

heating season. On the contrary, they can extract the heat from the conditioned spaces and inject it (again, in addition to their energy input) to the soil during the cooling season. Temperature values that are adequate to reach comfort levels in living spaces and advantageous for engineering applications (e.g., de-icing of infrastructures) can be achieved through this technology with a highly efficient use of primary energy. Traditionally, geothermal borehole heat exchangers have been exploited for this purpose. Recently, the use of energy piles has been increasingly spreading because of the savings in the installation costs related to their hybrid character and to the drilling process.

The EPs possess a twofold technological character that has drawn a dual related scientific interest in their behaviour. In fact, the energy performance of the energy piles can markedly vary for different *(i)* site layouts, *(ii)* foundation geometries, *(iii)* pipe configurations, and *(iv)* soil and foundation material properties. In addition, the geotechnical behaviour of the energy piles can strongly vary for different *(v)* restraint conditions and *(vi)* applied thermal loads. Consequently, these two fundamental aspects of the energy piles are interconnected and coupled through the thermal and mechanical responses of these foundations.

Over the years, a number of studies have investigated the thermal behaviour of vertical ground-coupled heat exchangers, focussing on the processes that occur inside (i.e., the tubes, infill material and fluid) and around (i.e., the surrounding soil) their domain. Analytical [1–11] and numerical [12–31] models of varying complexity have been developed for such purposes. Currently, various amounts of research have been increasingly performed for the analysis of the thermal behaviour of energy piles [32–49]. However, the three-dimensional, asymmetric and time-dependent characterisation of the thermal behaviour of such foundations, which involves the interaction between the fluid in the pipes, the pipes themselves, the pile and the surrounding soil, has often been considered in simplified ways that have been deepened only for specific case studies and have not been coupled with the mechanics of the problem. This latter aspect, i.e., the variation of the mechanical behaviour of both the foundation and the soil surrounding the energy piles due to thermal loads, has been investigated in recent years through several numerical studies in the field of civil engineering [50–60]. However, except for some of the very latest research [61,62], these studies generally simplified the numerical modelling of the complex thermal behaviour of the energy piles by imposing temperature variations or thermal powers to the entire modelled foundations, which were considered to be homogeneous solids, without the inner pipes and the circulating fluid. From a geotechnical and structural engineering point of view, this approach put the analyses on the side of safety (especially in the short-term) because the entire foundation undergoes the highest temperature variation and hence the maximum induced mechanical effect. However, from an energy engineering point of view, the physics governing the real problem has been markedly approximated. In particular, when dealing with models in which ground heat exchangers are coupled to the other building-plant sub-systems within a global thermodynamic and energetic analysis [63–65], the aforementioned simplifications may lead to inaccurate performance predictions and non-optimal design choices.

Energy piles, because of their bluffness, should be analysed as capacity systems capable of responding to a phase shift in a variation of the boundary conditions. More specifically, the thermal behaviour of the foundation should be investigated considering the complex pipes–pile–soil system as the heat exchange problem is governed by the temperature differences between these components. Together with these aspects, the coupled transient mechanical behaviour of the foundation should be analysed as it governs the bearing response for the superstructure. In this framework, looking at a thorough assessment of the interplay between the thermal and mechanical behaviour of energy piles, the present paper summarises the results of a series of 3-D numerical sensitivity analyses comprising the considered aspects for a single full-scale energy pile. This study is performed with reference to the features of the energy foundation of the Swiss Tech Convention Centre at the Swiss Federal Institute of Technology in Lausanne (EPFL), and investigates the roles of different *(i)* pipe configurations, *(ii)* foundation aspect ratios, *(iii)* mass flow rates of the working fluid, and *(iv)* fluid mixture compositions on the transient thermo-mechanical response of energy piles. This investigation focuses hence on the influence between the thermal and mechanical behaviours of energy piles under transient conditions considering different technical solutions applicable to such foundations. The adherence to physical reality characterising the numerical approach considered herein is corroborated by satisfying numerical predictions [66] of experimental tests [67,68] that have been recently performed at the site of interest.

The foundation is tested during its heating operation mode (the superstructure is heated while the ground is cooled). With respect to the considered design solutions, the energy considerations related to *(i)* the thermal response of the foundation in the short-term, *(ii)* the time constants for approaching the steady state conditions of the heat exchange and *(iii)* the heat transferred between the fluid in the pipes and the surrounding system are presented. Geotechnical aspects related to *(iv)* the stress distribution in the pile and *(v)* the displacements fields characterising the foundation depth are also considered.

In the following sections, the key features characterising the finite element modelling of the examined problem are first presented. The results of the numerical sensitivity analyses are then outlined. Finally, the thermo-mechanical behaviour of the energy piles and the related energy and geotechnical performances are discussed with reference to the simulated design solutions.

## 2. 3-D finite element modelling of an energy pile

### 2.1. The simulated site

The dimensions of the energy pile and the characteristics of the surrounding soil deposit considered in this study are those of an experimental site located at the Swiss Federal Institute of Technology in Lausanne (EPFL), under the recently built Swiss Tech Convention Centre. The experimental site includes a group of four energy piles installed below a corner of a heavily reinforced raft supporting a water retention tank. The foundation of the tank includes, besides the four energy piles, eleven other conventional piles that are not equipped as heat exchangers [67,68]. This study considers only one of the four energy piles with respect to a configuration denoted by a null head restraint and a null mechanical applied load on the top of the foundation, i.e., the one before the construction of the water tank. The energy pile is characterised by a height $H_{EP} = 28$ m and a diameter $D_{EP} = 0.90$ m (see Fig. 1). The pipes in the shallower 4 m are thermally insulated to limit the influence of the external climatic conditions on the heat exchange process. The characteristics of the soil deposit surrounding the piles (see again Fig. 1) are similar to those reported by Laloui et al. [53] as the considered energy foundation is placed in close proximity to the one referred in this study. The ground water table at the test site is at the top of the deposit. The upper soil profile consists of alluvial soil for a depth of 7.7 m. Below this upper layer, a sandy gravelly moraine layer is present at the depth between 7.7 and 15.7 m. Then, a stiffer thin layer of bottom moraine is present at a depth between 15.7 and 19.2 m. Finally, a molasse layer is present below the bottom moraine layer.

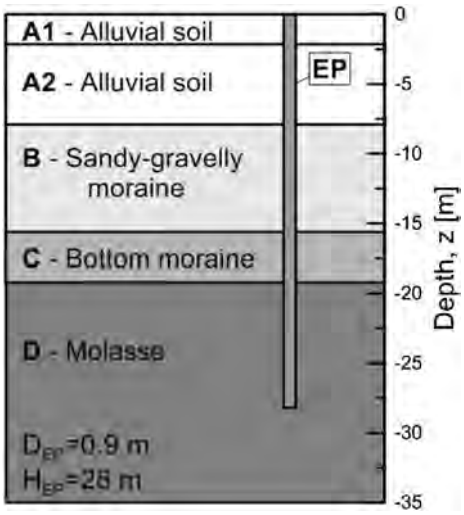


**Fig. 1.** Typical soil stratigraphy surrounding the Swiss Tech Convention Centre energy foundation.

### 2.2. Mathematical formulation and constitutive models

To develop a quantitative description of the response of the energy pile in the considered soil deposit under the mechanical and thermal loads, the following assumptions were made: *(i)* the soil layers were considered to be isotropic, fully saturated by water and assumed to be purely conductive domains with equivalent thermo-physical properties given by the fluid and the solid phases, *(ii)* both the liquid and the solid phases were incompressible under isothermal conditions, *(iii)* the displacements and the deformations of the solid skeleton were able to be exhaustively described through a linear kinematics approach in quasi-static conditions (i.e., negligible inertial effects), *(iv)* drained conditions were satisfied during the analysed loading processes, and *(v)* both the soil and energy pile behaved as linear thermo-elastic materials. Assumptions *(i–iii)* have been widely accepted in most practical cases. Hypotheses *(iv–v)* were considered to be representative of the analysed problem in view of the experimental evidence that was obtained through *in-situ* tests performed at the site [68,69]. Therefore, under these conditions, a coupled thermo-mechanical mathematical formulation has been employed in the following analyses.

The equilibrium equation can be written as

$$\nabla\cdot\sigma_{ij} + \rho g_i = 0 \tag{1}$$

where $\nabla\cdot$ denotes the divergence; $\sigma_{ij}$ denotes the stress tensor; $\rho$ represents the bulk density of the porous material, which includes the density of water $\rho_w$ and the density of the solid particles $\rho_s$, through the porosity $n$; and $g_i$ is the gravity vector. The stress tensor can be expressed in incremental form as

$$d\sigma_{ij} = C_{ijkl}(d\varepsilon_{kl} + \beta_{kl}dT) \tag{2}$$

where $C_{ijkl}$ is the stiffness tensor that contains the material parameters, i.e., the Young's modulus, $E$, and Poisson's ratio, $\upsilon$; $\varepsilon_{kl}$ is the total strain tensor; $\beta_{kl}$ is a tensor that contains the linear thermal expansion coefficient of the material, $\alpha$; and $T$ is the temperature.

As previously mentioned, the ground and the concrete filling of the EP were assumed to be purely conductive media. With these assumptions, the energy conservation equation reads

$$\rho c\frac{\partial T}{\partial t} - \nabla\cdot(\lambda\nabla T) = 0 \tag{3}$$

where $c$ is the specific heat (including water and solid components $c_w$ and $c_s$); $t$ is the time; $\lambda$ is the thermal conductivity (including water and solid components $\lambda_w$ and $\lambda_s$); and $\nabla$ represents the gradient. In equation (3), the first term represents the transient component of the internal energy stored in the medium and the second term represents the heat transferred by conduction (i.e., through Fourier's law). In the considered engineering application, the thermal properties of the fluid components were considered to be temperature dependent, whereas those of the solid components were considered to be temperature independent.

The energy conservation equation for the incompressible fluid flowing in the EP pipes can be written as

$$\rho_f c_f A_p\frac{\partial T_{bulk,f}}{\partial t} + \rho_f c_f A_p u_{f,i}\cdot\nabla\left(T_{bulk,f}\right) = \nabla\cdot\left[A_p\lambda_f\nabla\left(T_{bulk,f}\right)\right] + \dot{q}_p \tag{4}$$

where $\rho_f$, $c_f$, $A_p$, $T_{bulk,f}$, $u_{f,i}$, $\lambda_f$ are the density, specific heat, pipe cross sectional area, bulk temperature, longitudinal velocity vector and thermal conductivity of the operative fluid, respectively; $\dot{q}_p$ represents the heat flux per unit length exchanged through the pipe wall and is given by

$$\dot{q}_p = UP_p\left(T_{ext} - T_{bulk,f}\right) \tag{5}$$

where $U$ is an effective value of the pipe heat transfer coefficient, $P_p = 2\pi r_{int}$ is the wetted perimeter of the cross section, and $T_{ext}$ is the temperature at the outer side of the pipe. The overall heat transfer coefficient, including the internal film resistance and the wall resistance, can be obtained as follows:

$$U = \frac{1}{\frac{1}{h_{int}} + \frac{r_{int}}{\lambda_p}\ln\left(\frac{r_{ext}}{r_{int}}\right)} \tag{6}$$

where $h_{int} = Nu\lambda_f/d_h$ is the convective heat transfer coefficient inside the pipe, $\lambda_p$ is the thermal conductivity of the pipe, $r_{ext}$ and $r_{int}$ are the external and internal radii, respectively, $d_h = 4A_p/P_p$ is the hydraulic diameter, and $Nu$ is the Nusselt number. For a given geometry, $Nu$ is a function of the Reynolds, $Re$, and Prandtl, $Pr$, numbers, with

$$Nu = \max(3.66; Nu_{turb}) \tag{7.a}$$

$$Nu_{turb} = \frac{(f_D/8)(Re - 1000)Pr}{1 + 12.7\sqrt{f_D/8}\left(Pr^{\frac{2}{3}} - 1\right)} \tag{7.b}$$

$$f_D = \left[-1.8\log_{10}\left(\frac{6.9}{Re}\right)\right]^{-1} \tag{7.c}$$

where

$$Re = \frac{\rho f^u f^d h}{\mu_f} \quad Pr = \frac{\mu_f c_f}{\lambda_f}$$

Equation (7.b) is the Gnielinski formula [70] for turbulent flows; the friction factor, $f_D$, is evaluated through the Haaland equation [71], which is valid for very low relative roughness values.

### 2.3. 3-D finite element model features

The analyses presented in this study employed the software COMSOL Multiphysics [72], which is a finite element simulation environment. In the following sections, sensitivity analyses were conducted with respect to three different base-case models of a single energy pile equipped with a single U, a double U, and a W-shaped type configuration of the pipes. Extra-fine meshes of 107,087, 88,597 and 98,357 elements were used to characterise the models for the different foundations. Tetrahedral, prismatic, triangular, quadrilateral, linear and vertex elements were employed to describe the $50D_{EP}\cdot 2H_{EP}\cdot 2H_{EP}$ 3-D finite element models. Fig. 2 reports the features of a typical model utilised in the study with a focus on the mesh used to characterise the pile that was equipped with different pipe configurations. The energy pile was described by 49,824, 66,722, and 70,970 elements for the single U, double U, and W-shaped type configurations, respectively. The soil surrounding the pile was then characterised by the remaining 57,263, 21,875, and 27,387 elements for the various models. Tetrahedral elements were used near the joints of the pipes, whereas the remaining domain of the pile was covered by means of the swept method. The pipes were simulated with a linear entity in which the fluid was supposed to flow. In all of the cases, the centres of the pipes were placed at a distance of 12.6 cm from the boundary of the foundation. Fluid flow inside of the pipes and the associated convective heat transfer was simulated by an equivalent solid [73], which possessed the same heat capacity per unit volume (i.e., specific heat multiplied by bulk density) and thermal conductivity as the actual circulation fluid.

### 2.4. Boundary and initial conditions

Restrictions were applied to both the vertical and horizontal displacements on the base of the mesh (i.e., pinned boundary) and to the horizontal displacements on the sides (i.e., roller boundary). The initial stress state due to gravity in the pile and the soil was considered to be geostatic. The thermal boundary conditions allowed for the heat to flow through the vertical sides of the mesh and through the bottom of the mesh ($T_{soil} = 13.2$ °C). The initial temperatures in the pipes, energy pile and soil were set at $T_0 = 13.2$ °C, i.e., the average measured temperature at the considered site during winter. The fluid circulating inside the pipes (high-density polyethylene tubes) considered in the base-case models was water. The nominal velocity of the fluid inside the pipes was $u_f = 0.2$ m/s, and the inner diameter of the pipes was $\phi = 32$ mm. In all of the tests, the inflow temperature of the fluid was set at $T_{in} = 5$ °C, which referred to the operation of the energy foundation in winter. A thermal conductivity $\lambda_p = 0$ W/(mK) was imposed in the shallower 4 m of the pipes to simulate the thermal insulation of the ducts near the ground surface. The finite element mesh and the boundary conditions used in the simulations are shown in Fig. 2.

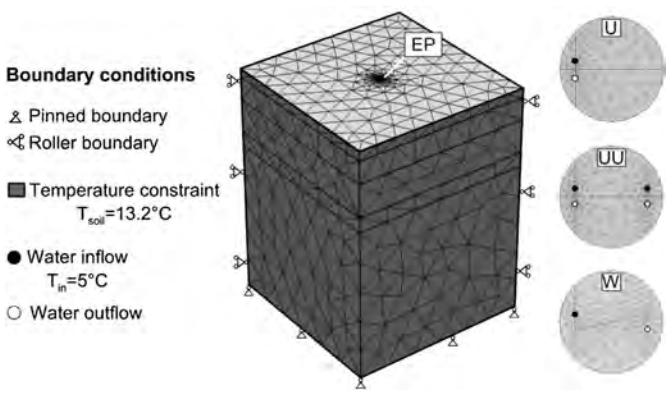


**Fig. 2.** Finite element mesh and boundary conditions used in the simulations.

### 2.5. Material properties

The soil deposit, energy pile and pipes properties were defined based on the literature review and in view of the technical documents related to the considered engineering project [53,67,69,74,75]. They are summarised in Table 1.

## 3. Thermo-mechanical sensitivity of the energy piles to the different technical solutions

The results of different numerical sensitivity analyses considering *(i)* various pipe configurations inside of the single energy pile, *(ii)* foundation aspect ratios, *(iii)* fluid flow rates inside the pipes and *(iv)* fluid compositions are presented in the following sections. The tests, performed through 3-D transient finite element simulations, occurred over 15 days in winter. This period has been proven to be sufficient to reach steady-state within the EP domain: consequently, the enthalpy drop of the fluid from the inlet to the outlet section of the pipes corresponded to the thermal power exchanged at the EP outer surface (the one in contact with the soil). Under such conditions, the heat capacity effects were negligible and the energy pile behaved as a typical heat exchanger that was characterised by an equivalent thermal resistance between the ducts and the soil. The classical effectiveness method for heat exchangers [76] was used to evaluate and compare the heat transfer process among the different EP configurations. The heat exchanger effectiveness, $\varepsilon_{he}$, is defined as

$$\varepsilon_{he} = \frac{T_{out} - T_{in}}{T_{s-p} - T_{in}} \tag{8}$$

where $T_{s-p}$ is the average temperature at the soil–pile interface.

Compressive stresses and strains were considered to be positive, as were the downward displacements (i.e., settlements).

### 3.1. Influence of the configuration of the pipes

The thermo-mechanical behaviour of a single energy pile equipped with a single U, a double U and W-shaped pipes was investigated.

Fig. 3 shows the axial distributions of the temperature for each type of configuration. As can be noted, no remarkable temperature variation characterised the shallower 4 m of the foundation because the pipes in this region were thermally insulated. After 15 days, the centre of the foundation equipped with single U, double U and W-shaped pipe configurations underwent an average cooling of $\Delta T = T - T_0 = -3.5$, $-5.5$, and $-5$ °C, respectively. The highest temperature variation was reached with the double U-shaped geometry of pipes because it involved the highest quantity of cold water in the heat exchange process. A more pronounced cooling of the bottom part of the pile was observed due to the lower thermal conductivity of the molasse layer, which induced a lower heat exchange with the foundation. The temperature distribution along the axial foundation depth did not remarkably vary in all of the cases between 7 and 15 days, indicating that the thermal conditions

**Table 1**
Material properties of the soil deposit, energy pile, and pipes.

| | $E$ [MPa] | $\nu$ [−] | $n$ [−] | $\rho_s$ [kg/m$^3$] | $c_s$ [J/(kg K)] | $\lambda_s$ [W/(m K)] | $\alpha$ [1/K] |
|---|---|---|---|---|---|---|---|
| **Soil layer** | | | | | | | |
| A1 | 190 | 0.22 | 0.1 | 2769 | 880 | 1.8 | $0.33 \times 10^{-5}$ |
| A2 | 190 | 0.22 | 0.1 | 2769 | 880 | 1.8 | $0.33 \times 10^{-5}$ |
| B | 84 | 0.4 | 0.35 | 2735 | 890 | 1.8 | $0.33 \times 10^{-4}$ |
| C | 90 | 0.4 | 0.3 | 2740 | 890 | 1.8 | $0.33 \times 10^{-4}$ |
| D | 3000 | 0.2 | 0.1 | 2167 | 923 | 1.11 | $0.33 \times 10^{-6}$ |
| **Energy pile and pipes** | | | | | | | |
| Concrete | 28,000 | 0.25 | 0.1 | 2500 | 837 | 1.628 | $1 \times 10^{-5}$ |
| HDPE | – | – | – | – | – | 0.42 | – |

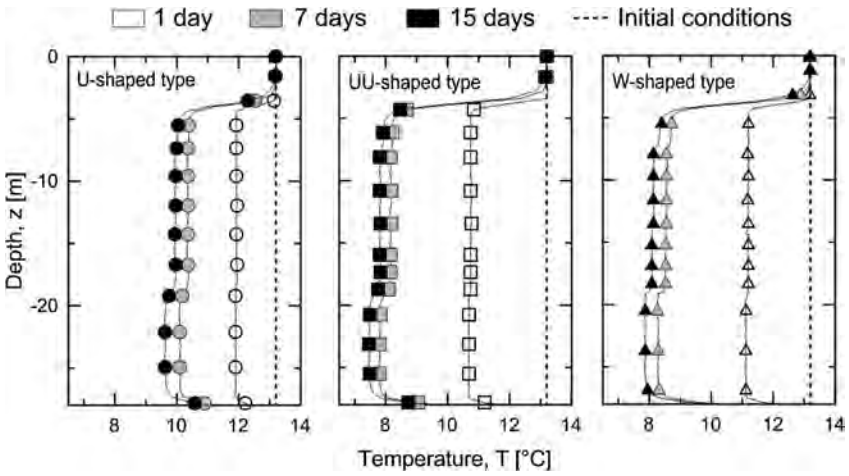


**Fig. 3.** Axial temperature distributions for the different pipe configurations.

inside the pile were already close to steady state during the first week of operation.

The axial distributions of stress induced by the above-described temperature variations are shown in Fig. 4 (the initial stress distribution due to the foundation body load was subtracted). Maximum values of the stress $\sigma_{v,th} = -800$, $-1400$ and $-1300$ kPa were observed along the axial depths of the foundation for the single U, double U, and W-shaped pipe configurations, respectively. These results were consistent with the previously observed data because the configurations of the pipes that led to the greatest negative temperature variations inside the pile were the configurations for which the greatest stresses were observed from the foundation thermal contractions. The magnitude of the stress induced by the temperature variation in the energy pile equipped with the single U-shaped pipe configuration was close to the one characterising the results obtained by Gashti et al. [62] for a single energy pile tested in winter conditions with the same type of pipe configuration.

Fig. 5 shows the axial distribution of the vertical displacements for each configuration. Consistent with the distributions of the

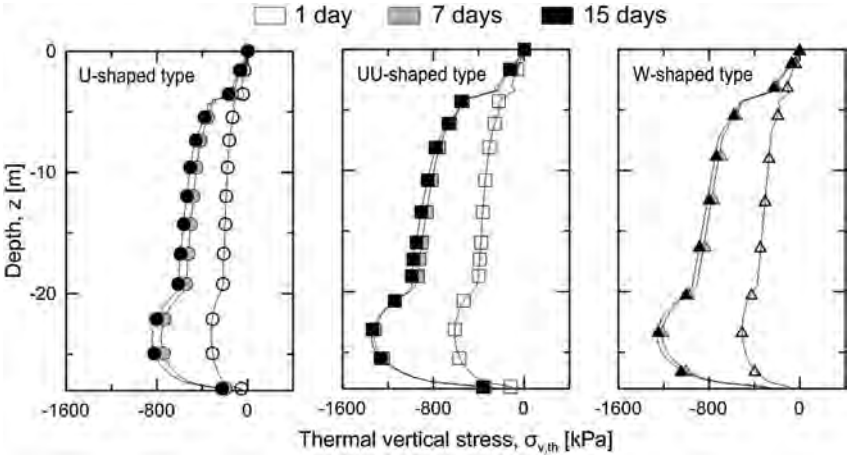


**Fig. 4.** Axial distributions of the thermal vertical stresses for the different pipe configurations.

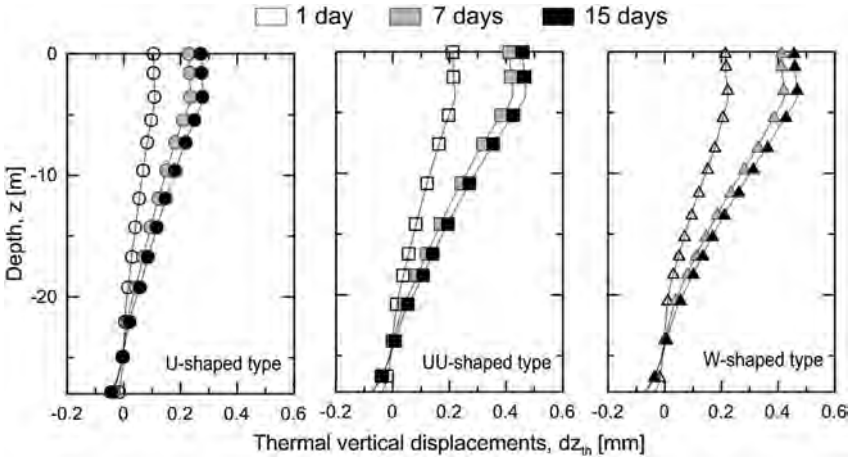


**Fig. 5.** Axial distributions of the thermal vertical displacements for the different pipe configurations.

temperature and stress, the greatest effect in terms of the displacement of the cold flow within the tubes was observed for the pile with the double U-shaped pipe configuration, whereas the smallest effect was observed in the foundation with the single U-shaped pipe configuration. Maximum pile settlements $dz_{th} = 0.28$, 0.47 and 0.46 mm were observed for the energy pile equipped with the single U, double U, and W-shaped pipe configurations, respectively. The null point, which represents the plane where zero thermally induced displacement occurs in the foundation [69], was close to the bottom of the energy pile for all of the cases. This occurrence was similarly observed by Gashti et al. [62].

The temperature trends of the water circulating in the pipes are reported in Fig. 6. As can be observed, the water temperature linearly increased along the flow direction. However, the slight changes of the slope of the curves indicated that the increase was not uniform because the spatial progressive increase of the water temperature in the pipe reduced the heat transfer potential with the soil, which thus led to slower temperature increases. The fluid outflow temperatures, $T_{out}$, were higher for the single U pipe configuration with respect to the double U configuration, and this can be attributed to a thermal interference that occurred in the latter solution between the two U pipes within the pile. The highest temperature increase was obtained for the W-shaped pipe configuration, according to the study proposed by Gao et al. [34].

The trends of the thermal power extracted from the ground for the energy pile equipped with the different considered pipe configurations for the entire duration of the tests is reported in Fig. 6. Complementary data referring to the end of the simulations (15 days) are finally summarised in Table 2.

A decrease of the thermal power extracted from the ground along the foundation depth, $\dot{Q}/H_{EP}$, was observed throughout all of the tests (cf. Fig. 7) that was consistent with the temperature decrease that occurred at the soil–pile interface; however, as already noted, the time evolution of the extracted thermal power almost reached steady-state after one week of continuous operation. The highest levels of energy extraction were obtained through the double U and W-shaped pipe solutions, whereas lower amounts of energy were removed from the ground through the single U-shaped pipe configuration. These results are quantitatively reported in Table 2, which shows that after 15 days, the energy pile equipped with the double U-shaped pipes had a 57% higher heat transfer rate than what was obtained through a single U-shaped pipe configuration; on the other hand, the former design solution was only 2% more efficient than the one with the W-shaped pipe. In conclusion, the W-shaped pipe configuration should be considered to be the best trade-off among the design solutions analysed in this section, owing to *(i)* a significantly higher energy extraction with respect to the single U-shaped pipe configuration, which justifies

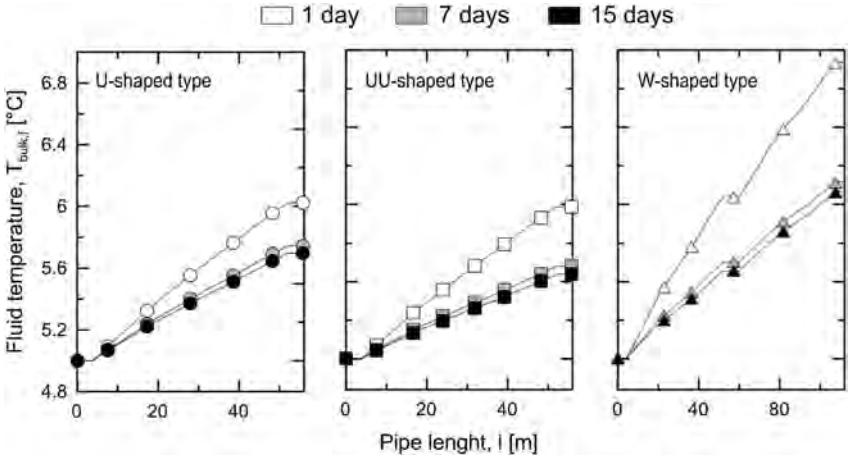


**Fig. 6.** Distributions of the water temperature in the pipes for the different configurations.

**Table 2**
Thermal performances of the energy piles for the different pipe configurations.

| Pipes configuration | $T_{out}$ [°C] | $\Delta T$ [°C] | $T_{s-p}$ [°C] | $\varepsilon_{he}$ [−] | $\dot{V}$ [l/min] | $\dot{Q}/H_{EP}$ [W/m] |
|---|---|---|---|---|---|---|
| Single U-shaped | 5.70 | 0.70 | 10.73 | 0.122 | 9.7 | 16.9 |
| Double U-shaped | 5.55 | 0.55 | 9.06 | 0.135 | 19.3 | 26.5 |
| W-shaped | 6.08 | 1.08 | 9.15 | 0.260 | 9.7 | 26.1 |

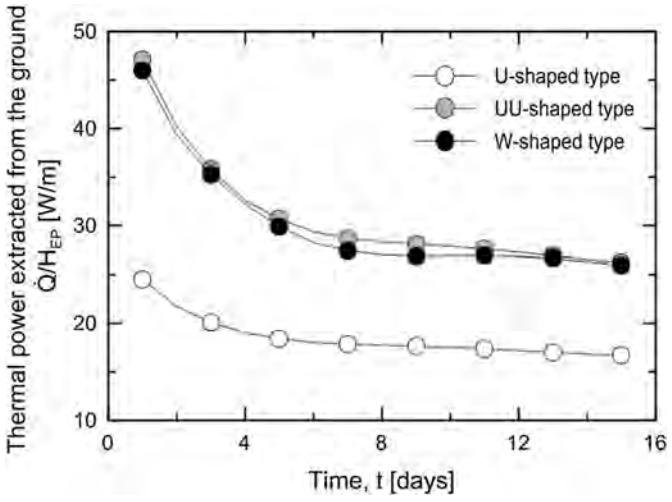


**Fig. 7.** Trend of the thermal power extracted from the ground for the different pipe configurations.

its higher installation cost; and *(ii)* a negligibly lower energy extraction with respect to the double U-shaped pipe configuration that was operated at half of the volumetric flow rate, $\dot{V}$, that was globally needed for the latter solution (thus entailing significantly less pumping power). The reason for such similar thermal behaviour between the two solutions must be determined by the low effectiveness of these short ground-coupled heat exchangers, $\varepsilon_{he}$, that was defined in equation (8); more specifically, a significant departure from the linear trend of the effectiveness versus heat exchanger surface (which is double for the W-shaped pipe configuration with respect to each of the two U-legs) towards saturation was not obtained in the tested configurations.

### 3.2. Influence of the foundation aspect ratio

The thermo-mechanical behaviour of a single energy pile with aspect ratios $AR = H_{EP}/D_{EP} = 10$, 20 and 40 ($D_{EP} = 0.9$ m) was investigated in the present section. The analyses were performed with respect to the previously considered pipe configurations, and, in each case, the results were compared to those of the energy pile that was characterised by the nominal aspect ratio $AR = 31$, which was already simulated in Section 3.1.

Fig. 8 shows the axial temperature distributions for each pile aspect ratio and pipe configuration. The foundation depth was considered in a dimensionless form by dividing it by the total height of the pile, $H_{EP}$. Different temperature distributions along the vertical coordinate were observed for the various aspect ratios depending upon the thermal properties of the various soil layers and, above all, on the relative influence of the upper adiabatic 4 m. As previously observed, the highest temperature variations (and therefore the highest axial stresses and displacements variations) were obtained for the energy pile equipped with the double U-shaped pipes.

The axial distributions of the thermally induced stress in the pile are shown in Fig. 9. Lower and more homogeneous distributions of the vertical axial stress were observed for the piles with lower aspect ratios $AR = 9$ and 18, whereas higher and less homogeneous distributions were obtained for the foundation characterised by the nominal dimensions ($AR = 31$) and for the one with the highest aspect ratio $AR = 36$. This result was due to *(i)* the different bearing behaviour that characterised the foundation in the various considered cases, i.e., predominantly frictional results were observed until an approximate depth of 20 m and a more pronounced end-bearing characteristic was observed from a depth of 20 m on and *(ii)* due to the impact of the thermal properties of the various soil layers on the heat exchange process and on the related thermally induced stress. Upper bound values of the axial stress $\sigma_{v,th} = -926$, $-1531$ and $-1513$ kPa were reached in the bottom half of the deeper and more constrained foundation for the single U,

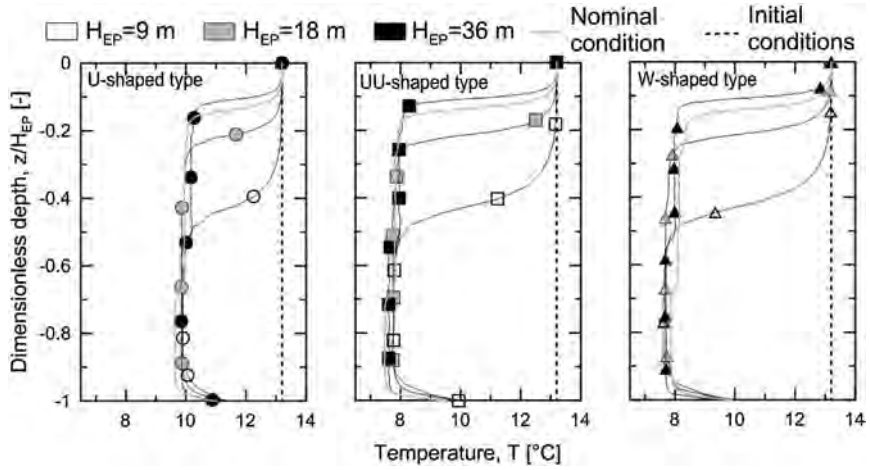


**Fig. 8.** Axial temperature distributions for the different pile aspect ratios.

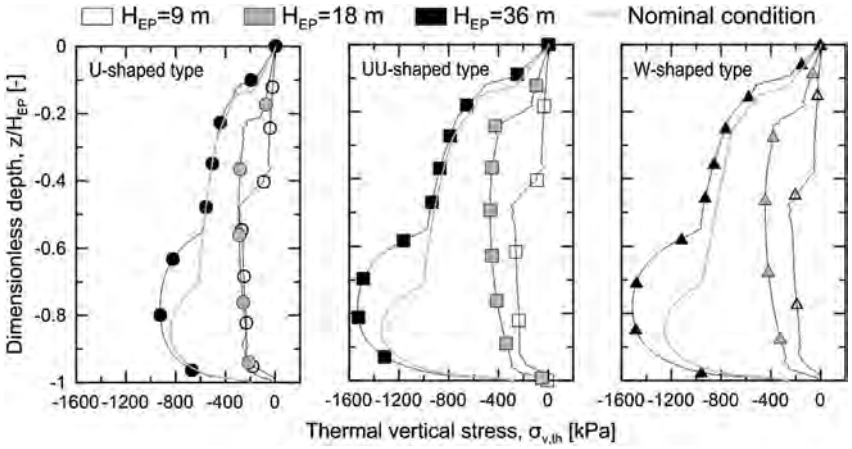


**Fig. 9.** Axial distributions of the thermal vertical stresses for the different pile aspect ratios.

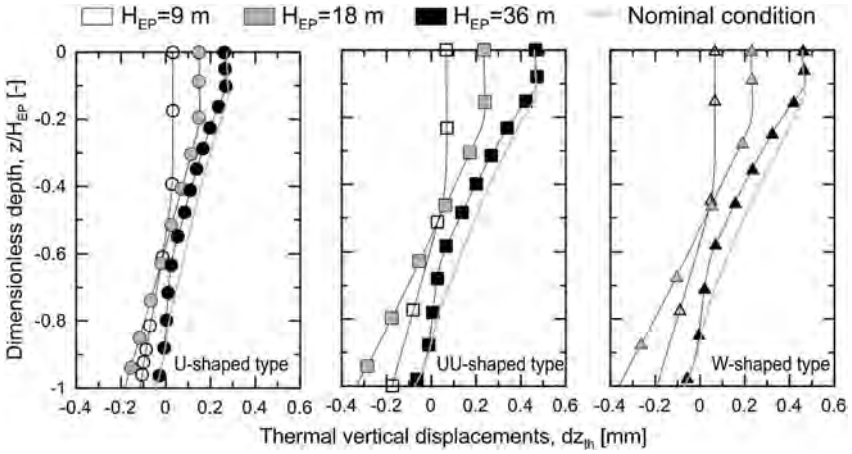


**Fig. 10.** Axial distributions of the thermal vertical displacements for the different pile aspect ratios.

double U, and W-shaped pipe configurations, respectively. Lower bound values of the axial stress $\sigma_{v,th} = -181$, $-300$ and $-261$ kPa were reached close to the centre of the shallower and less constrained foundation for the same pipe configurations.

The effect of the different foundation constraints and thermal properties of the various soil layers can also be observed in Fig. 10, which showed the thermal vertical displacements along the dimensionless foundation depths for the different aspect ratios. The null point location was close to the geometrical centre of the foundation for the aspect ratios $AR = 9$ and 18, whereas it was close to the bottom for the aspect ratios $AR = 31$ and 36. This result outlines the more pronounced end-bearing behaviour of the

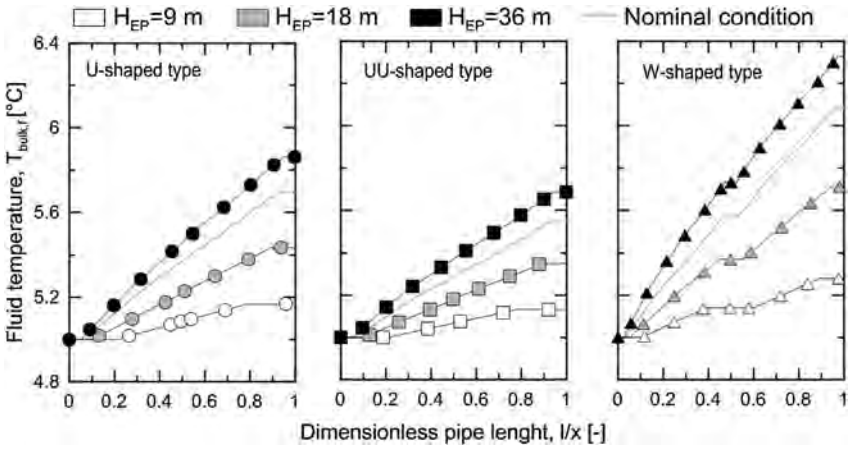


**Fig. 11.** Distributions of the water temperature in the pipes for the different pile aspect ratios.

**Table 3**
Thermal performances of the energy piles for the different aspect ratios.

| $AR$ [-] | $T_{out}$ [°C] | $\Delta T$ [°C] | $T_{s-p}$ [°C] | $\varepsilon_{he}$ [−] | $\dot{V}$ [l/min] | $\dot{Q}/H_{EP}$ [W/m] |
|---|---|---|---|---|---|---|
| **Single U-shaped pipe** | | | | | | |
| 10 | 5.17 | 0.17 | 10.85 | 0.028 | 9.7 | 12.5 |
| 20 | 5.44 | 0.44 | 10.71 | 0.077 | 9.7 | 16.5 |
| 31.1[a] | 5.70 | 0.70 | 10.73 | 0.122 | 9.7 | 16.9 |
| 40 | 5.86 | 0.86 | 10.65 | 0.152 | 9.7 | 16.1 |
| **Double U-shaped pipes** | | | | | | |
| 10 | 5.14 | 0.14 | 9.20 | 0.032 | 19.3 | 20.3 |
| 20 | 5.35 | 0.35 | 9.05 | 0.086 | 19.3 | 26.3 |
| 31.1[a] | 5.55 | 0.55 | 9.06 | 0.135 | 19.3 | 26.5 |
| 40 | 5.69 | 0.69 | 8.80 | 0.182 | 19.3 | 25.9 |
| **W-shaped pipe** | | | | | | |
| 10 | 5.28 | 0.28 | 9.02 | 0.070 | 9.7 | 21.0 |
| 20 | 5.71 | 0.71 | 8.94 | 0.180 | 9.7 | 26.6 |
| 31.1[a] | 6.08 | 1.08 | 9.15 | 0.260 | 9.7 | 26.1 |
| 40 | 6.33 | 1.33 | 8.82 | 0.347 | 9.7 | 24.9 |

[a] Base case.

foundation for depths greater than 20 m, where the molasse layer was found and a higher fraction of the load was transferred to the pile toe. Upper bound values of the settlements $dz_{th} = 0.3$, 0.7 and 0.65 mm were observed for the deeper foundation for the single U, double U, and W-shaped pipe configurations, respectively. Lower bound values of the settlements $dz_{th} = 0.27$, 0.47 and 0.47 mm were observed for the shallower foundation that was equipped with the same pipe configurations.

The distribution of water temperature inside the pipes for the entire duration of the tests and the useful data related to the energy performance of the piles at the end of the analyses are finally summarised in Fig. 11 and Table 3, respectively. The curvilinear coordinate following the pipe axis was expressed in dimensionless form by dividing it by the total length of the pipe, $x$. As can be observed in Fig. 11, the temperature of the operative fluid in the pipes increased with the aspect ratio of the pile, obviously due to the increase in the heat transfer surface. The results of the simulations conducted at the nominal aspect ratio were consistent with the other results, as observed by the fact that the thermal power that was extracted from the ground with the double U-shaped pipes was the largest among the analysed solutions and was followed, in order, by the pile equipped with the W and single U-shaped pipes (cf. Table 3). A doubling of the foundation aspect ratio from 10 to 20 involved an increase of the thermal power extraction between 152% and 170% depending on the configuration of the pipes (the thermally uninsulated surface of the pile was increased by 172%), whereas a doubling from 20 to 40 resulted in a lower relative increase between 87% and 100% (the uninsulated surface was increased by 127%), which can be attributed to the tendency of the heat exchanger to become saturated with the increase in the heat transfer surface.

### 3.3. Influence of the fluid flow rate circulating in the pipes

The thermo-mechanical behaviour of a single energy pile characterised by different fluid flow rates circulating in the pipes was investigated in the present section. Because the fluid flow rate can change both by a variation of the tube diameter, $\phi$, and by the fluid velocity, $u_f$, the following numerical analyses considered both options through two different series of tests. First, the response of the energy pile equipped with pipes of different diameters with water flowing at a constant velocity was considered. Then, the response of the energy pile equipped with tubes of the same diameter but that were characterised by different velocities of the circulating fluid was investigated. The analyses were performed with respect to the previously considered pipe configurations, and in each case, the results were compared to those of the energy pile characterised by the nominal features.

#### 3.3.1. Pipe diameter variations

The axial temperature distributions obtained for the varying pipes diameters ($\phi = 25$ and 40 mm) with respect to the nominal conditions ($\phi = 32$ mm) and for the different pipe configurations are shown in Fig. 12. A significant decrease of the pile axial temperature with respect to nominal conditions (approximately 1 °C) was observed only for the W-shaped pipe configuration and for the pipe with the largest diameter (and therefore with the highest flow rate).

The uniform temperature distributions along the foundation depth led to small variations of the axial stress distributions for the different pipe diameters and configurations. In accordance with the temperature profile, the more pronounced variations were noted for the energy pile equipped with the W-shaped pipe where the use of the tubes with diameter $\phi = 40$ mm involved an increase of approximately −200 kPa of axial vertical stress with respect to the nominal conditions (cf. Fig. 13).

The distribution of the water temperature inside the pipes after 15 days and the trend of thermal power extracted from the ground

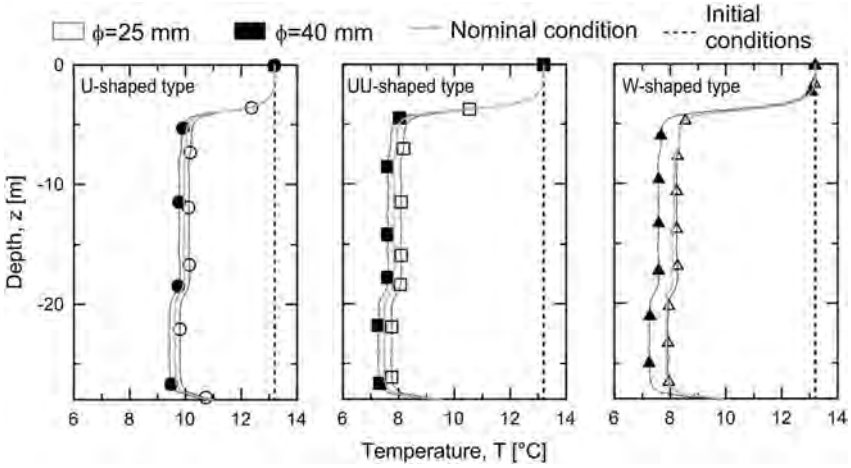


**Fig. 12.** Axial temperature distributions for the different pipe diameters.

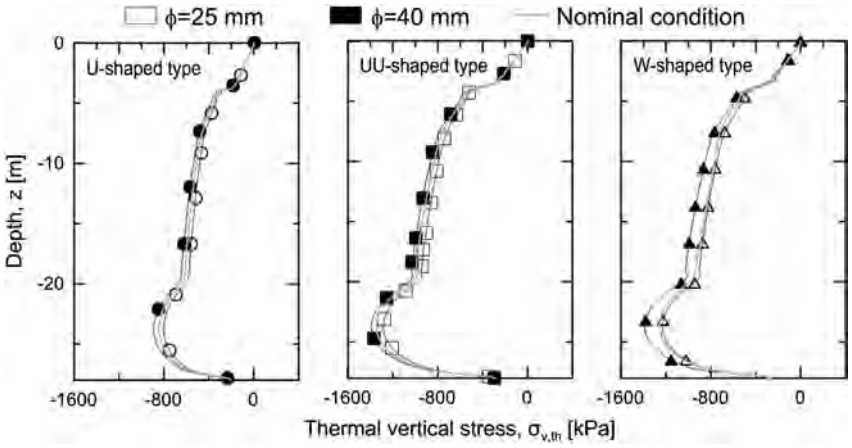


**Fig. 13.** Axial distributions of the vertical stress for the different pipe diameters.

for the entire duration of the tests are reported Fig. 14 as a function of the pipe diameters. Complementary data referring to the end of the simulations are summarised in Table 4.

Fig. 14 showed an increase in the outflow temperature when the diameter of the pipe was reduced, and this was attributed to the subsequent decrease in the flow rate. The most important effect that was observed by the variation of the pipe diameters was with the W-shaped pipe. The trend of thermal power extracted from the ground showed that besides its decay with time, up to 10% of the heat transfer rate was gained when the diameter of the pipes was increased from 25 to 40 mm (cf. Table 4).

### 3.3.2. Fluid velocity variations

The axial temperature distributions obtained by varying the water velocities in the pipes ($u_f = 0.5$ and 1 m/s) with respect to the nominal condition ($u_f$ = 0.2 m/s) and for the different pipe configurations are shown in Fig. 15. A significant lowering of the pile axial temperature with respect to the nominal conditions (approximately 1 °C) was observed for only the W-shaped pipe configuration, where the fluid velocity was increased from 0.2 to 0.5 m/s.

In accordance with the uniform temperature distributions along the foundation depth that were observed for the piles characterised by the single U and double U-shaped pipes, no remarkable variations of the axial stress distributions were noted in Fig. 16. In addition to the more pronounced variations with respect to the response of the foundation with nominal features, higher fluid velocities $u_f$ = 0.5 or 1 m/s involved an increase of approximately −200 kPa of axial vertical stress for the W-shaped pipe configuration.

The distribution of water temperature inside the pipes after 15 days and the trend of thermal power extracted from the ground for

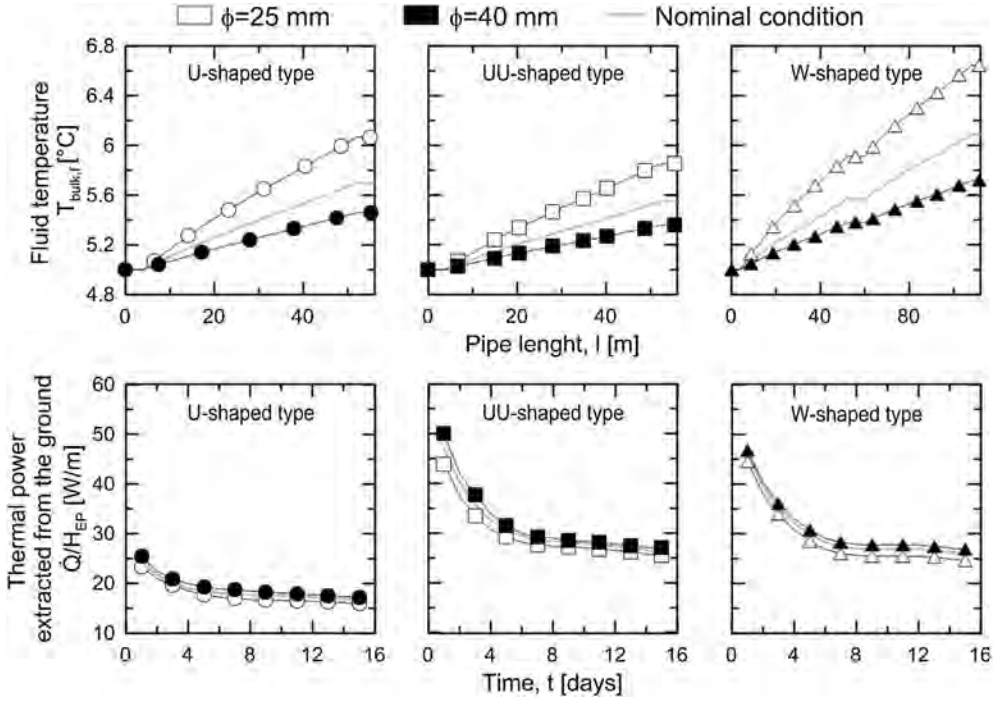


**Fig. 14.** Distributions of the water temperatures in the pipes for the different pipe diameters and the relative trends of the thermal power extracted from the ground.

**Table 4**
Thermal performances of the energy piles for the different pipe diameters.

| $\phi$ [mm] | $T_{out}$ [°C] | $\Delta T$ [°C] | $T_{s-p}$ [°C] | $\varepsilon_{he}$ [−] | $\dot{V}$ [l/min] | $\dot{Q}/H_{EP}$ [W/m] |
|---|---|---|---|---|---|---|
| **Single U-shaped pipe** | | | | | | |
| 25 | 6.07 | 1.07 | 10.67 | 0.189 | 5.9 | 15.8 |
| 32[a] | 5.70 | 0.70 | 10.73 | 0.122 | 9.7 | 16.9 |
| 40 | 5.46 | 0.46 | 10.44 | 0.085 | 15.1 | 17.3 |
| **Double U-shaped pipes** | | | | | | |
| 25 | 5.85 | 0.85 | 9.03 | 0.211 | 11.8 | 25.0 |
| 32[a] | 5.55 | 0.55 | 9.06 | 0.135 | 19.3 | 26.5 |
| 40 | 5.36 | 0.36 | 8.67 | 0.098 | 30.2 | 27.1 |
| **W-shaped pipe** | | | | | | |
| 25 | 6.64 | 1.64 | 9.25 | 0.386 | 5.9 | 24.2 |
| 32[a] | 6.08 | 1.08 | 9.15 | 0.260 | 9.7 | 26.1 |
| 40 | 5.72 | 0.72 | 8.56 | 0.201 | 15.1 | 27.0 |

[a] Base case.

the entire duration of the tests are reported in Fig. 17 as a function of the fluid velocities in the pipes. Complementary data referring to the end of the simulations are summarised in Table 5.

Fig. 17 showed a decrease in the outflow temperature when the water velocity in the pipes was increased, and this can be attributed to the increase in the flow rate. The trend of thermal power extracted from the ground showed that despite its typical decay with time, a sensible growth of the heat transfer efficiency was observed when the fluid velocity increased (cf. Table 5). In fact, the increase of the water velocity in the pipes from 0.2 to 0.5 m/s created an increase of approximately 7% in the heat transfer rate and a decrease from 0.2 to 1 m/s resulted in an increase of approximately 11%. These variations depended upon the configuration of the pipes, and the most relevant effects were observed for the W-shaped pipe configuration.

### 3.4. Influence of the operating fluid composition

Antifreeze is a chemical additive that lowers the freezing point of a water-based liquid. In pipes, it is often useful to insert an antifreeze liquid mixed with water to avoid technical problems especially when dealing with foundation working conditions characterised by very low temperature regimes.

The behaviour of a single energy pile with antifreeze additives of MEG 25 and MEG 50 (mixtures with 25% and 50% of mono-ethylene glycol in water, respectively) in the circulating fluid in the pipes was investigated in the present section. The analyses were performed with respect to the previously considered pipe configurations, and, in each case, the results were compared to those of the energy pile with water circulating in the pipes.

The thermal properties of MEG 25 and MEG 50 are reported in Table 6.

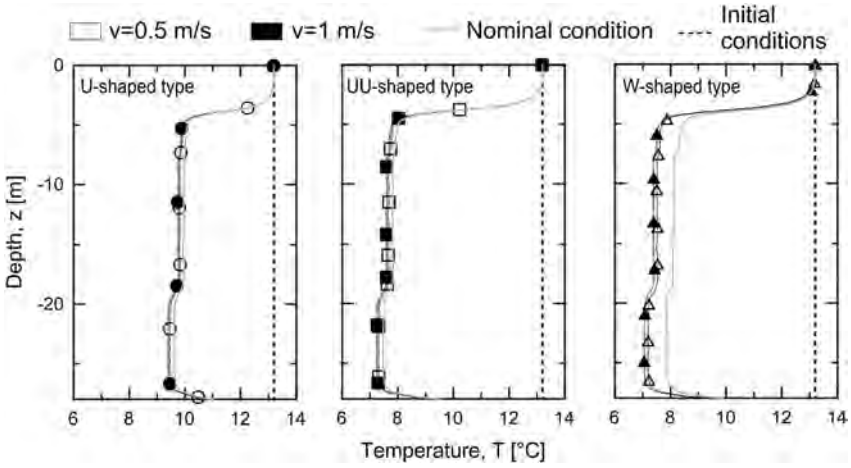


**Fig. 15.** Axial temperature distributions for the different water velocities.

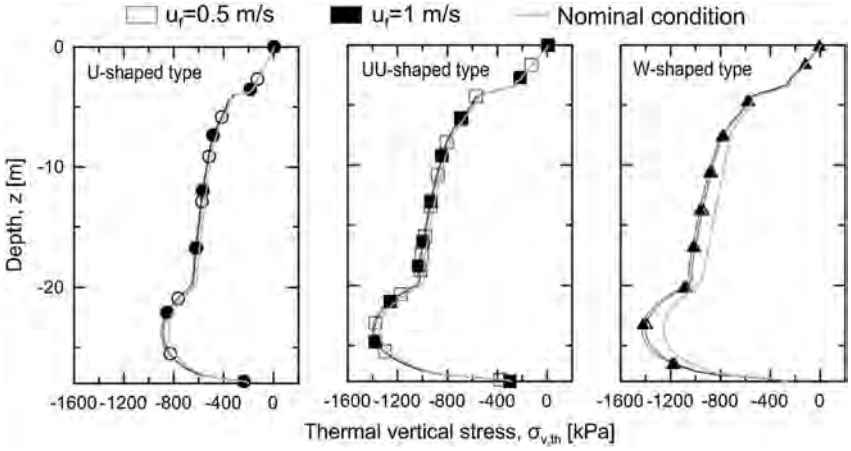


**Fig. 16.** Axial distributions of the thermal vertical stress for the different water velocities.

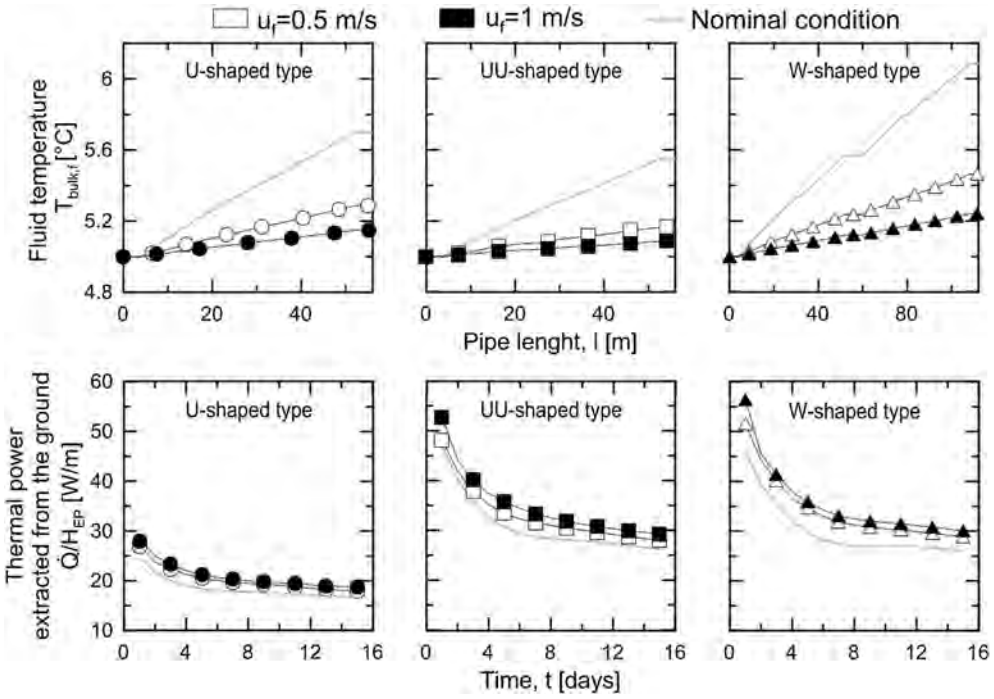


**Fig. 17.** Distributions of the water temperature in the pipes for the different water velocities and the relative trends of the rate of energy extraction from the soil.

Fig. 18 shows the axial temperature distributions that were obtained along the foundation depth with the different heat carrier fluids.

By varying the working fluid, no appreciable differences in the pile axial temperature distributions were observed. Therefore, the mechanical response of the foundation was not expected to markedly vary in terms of the stress or displacements.

The distribution of the operative fluid temperature inside the pipes after 15 days and the trends of thermal power extracted from the ground for the entire duration of the tests are reported in Fig. 19 as a function of the liquid circulating in the pipes. Complementary data referring to the end of the simulations are summarised in Table 7. The use of the antifreeze liquids did not appreciably affect the temperature of the fluid in the pipes, but it did induce variations in the performance of the system energy due to the lower specific heat of the medium.

**Table 5**
Energy performances for the different water velocities circulating inside of the pipes.

| $u_f$ [m/s] | $T_{out}$ [°C] | $\Delta T$ [°C] | $T_{s-p}$ [°C] | $\varepsilon_{he}$ [−] | $\dot{V}$ [l/min] | $\dot{Q}/H_{EP}$ [W/m] |
|---|---|---|---|---|---|---|
| **Single U-shaped pipe** | | | | | | |
| 0.2[a] | 5.70 | 0.70 | 10.73 | 0.122 | 9.7 | 16.9 |
| 0.5 | 5.29 | 0.29 | 10.47 | 0.052 | 24.1 | 17.2 |
| 1 | 5.15 | 0.15 | 10.41 | 0.028 | 48.3 | 18.1 |
| **Double U-shaped pipes** | | | | | | |
| 0.2[a] | 5.55 | 0.55 | 9.06 | 0.135 | 19.3 | 26.5 |
| 0.5 | 5.23 | 0.23 | 8.71 | 0.061 | 48.3 | 27.4 |
| 1 | 5.12 | 0.12 | 8.67 | 0.033 | 96.5 | 29.0 |
| **W-shaped pipe** | | | | | | |
| 0.2[a] | 6.08 | 1.08 | 9.15 | 0.260 | 9.7 | 26.1 |
| 0.5 | 5.46 | 0.46 | 8.51 | 0.132 | 24.1 | 27.9 |
| 1 | 5.24 | 0.24 | 8.38 | 0.071 | 48.3 | 29.0 |

[a] Base case.

Table 7 shows that a 25% concentration of MEG in water created a decrease of up to 6% in the heat transfer rate and that a 50% concentration of MEG created a decrease up to 11% with respect to the nominal conditions with pure water.

## 4. Concluding remarks

This paper summarises the results of a series of numerical simulations that were performed to investigate the effects of different design solutions (i.e., different pipe configurations, aspect ratios of the foundation, fluid flow rates circulating in the pipes, and fluid mixture compositions) on the energy and geotechnical performance of the energy piles. The study indicated that;

- The configuration of the pipes was the most important factor in the characterisation of the thermo-mechanical behaviour of the energy piles. It was observed that the W-shaped pipe configuration resulted in an increase of up to 54% in the heat transfer rate compared with the single U-shaped configuration at the same flow rate. The double U-shaped pipe configuration, which

**Table 6**
Thermal properties of MEG 25 and MEG 50.

| $T$ [°C] | $\rho_f$ [kg/m$^3$] | $c_f$ [J/(kg K)] | $\lambda_f$ [W/(m K)] | $\mu_f$ [Pa s] |
|---|---|---|---|---|
| **MEG 25** | | | | |
| −10 | 1048 | 3713 | 0.477 | $3.186 \times 10^{-3}$ |
| −5 | 1046 | 3719 | 0.481 | $2.704 \times 10^{-3}$ |
| 0 | 1045 | 3726 | 0.485 | $2.314 \times 10^{-3}$ |
| 5 | 1044 | 3734 | 0.489 | $1.995 \times 10^{-3}$ |
| 10 | 1042 | 3742 | 0.493 | $1.733 \times 10^{-3}$ |
| **MEG 50** | | | | |
| −10 | 1094 | 3201 | 0.413 | $5.316 \times 10^{-3}$ |
| −5 | 1092 | 3221 | 0.412 | $4.428 \times 10^{-3}$ |
| 0 | 1090 | 3240 | 0.411 | $3.723 \times 10^{-3}$ |
| 5 | 1087 | 3260 | 0.410 | $3.157 \times 10^{-3}$ |
| 10 | 1084 | 3280 | 0.408 | $2.700 \times 10^{-3}$ |

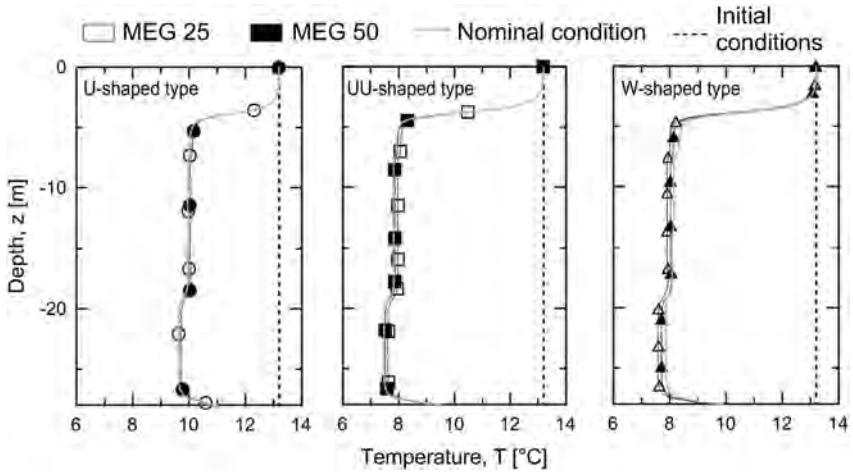


**Fig. 18.** Axial temperature distributions for the different operative fluids.

possessed a double flow rate with respect to the other configurations, resulted in the highest cooling of the concrete with the greatest related stress and displacement distributions. Therefore, it was considered to be a less advantageous solution with respect to the W-shaped pipe configuration both from a thermo-hydraulic and a geotechnical point of view.

- The increase of the foundation aspect ratio resulted in an approximately linear increase of the exchanged heat that was independent from the configuration of the pipes. However, a lengthening or shortening of the energy pile resulted in markedly diverse responses of the foundation to the thermo-mechanical loads, depending on the impact that the different mechanical and thermal properties of the surrounding soil layers may have had on the bearing response of the pile. In the considered cases, a lower and more homogeneous variation of stresses and displacements along the foundation depth was evidenced for the lower energy pile aspect ratios (i.e., $AR = 9$ and 18), whereas higher and less homogeneous evolutions were observed for the higher aspect ratios (i.e., $AR = 31$ and 36).
- An increase of up to 11% in the heat transfer rate was obtained by increasing the fluid flow rate (more specifically, increasing the water velocity from 0.2 to 1 m/s) with only slight differences in the results for the different pipe configurations (more evident variations were observed for the W-shaped pipe configuration). No remarkable variations of the vertical stress (and related strain and displacement) distributions in the foundation were observed with the variation in the fluid flow rates.
- Low concentrations of antifreeze that were mixed with water in the pipes did not markedly affect the energy performance of the pile with respect to the nominal case where pure water was

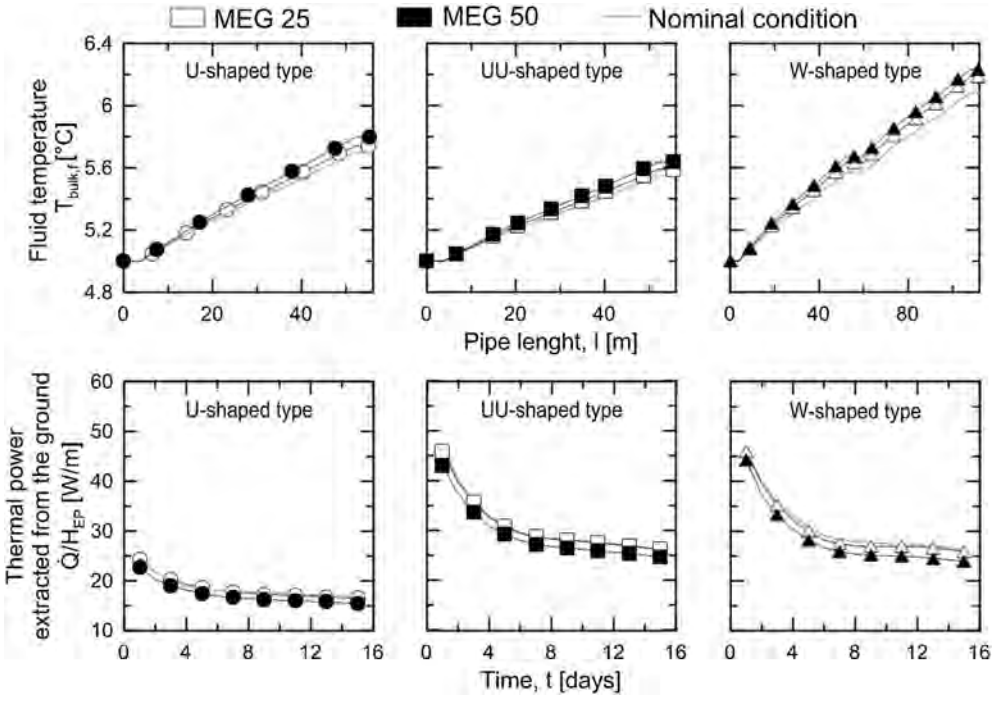


**Fig. 19.** Distributions of the operative fluid temperatures in the pipes and the relative trends of the thermal power extracted from the ground.

**Table 7**
Energy performances for the different operative liquids.

| Type of antifreeze | $T_{out}$ [°C] | $\Delta T$ [°C] | $T_{s-p}$ [°C] | $\varepsilon_{he}$ [−] | $\dot{V}$ [l/min] | $\dot{Q}/H_{EP}$ [W/m] |
|---|---|---|---|---|---|---|
| **Single U-shaped pipe** | | | | | | |
| Pure water[a] | 5.70 | 0.70 | 10.73 | 0.122 | 9.7 | 16.9 |
| MEG 25 | 5.74 | 0.74 | 10.59 | 0.132 | 10.1 | 18.6 |
| MEG 50 | 5.80 | 0.80 | 10.65 | 0.141 | 10.5 | 20.9 |
| **Double U-shaped pipes** | | | | | | |
| Pure water[a] | 5.55 | 0.55 | 9.06 | 0.135 | 19.3 | 26.5 |
| MEG 25 | 5.59 | 0.59 | 8.96 | 0.148 | 20.2 | 29.6 |
| MEG 50 | 5.64 | 0.64 | 8.94 | 0.161 | 21.0 | 33.4 |
| **W-shaped pipe** | | | | | | |
| Pure water[a] | 6.08 | 1.08 | 9.15 | 0.260 | 9.7 | 26.1 |
| MEG 25 | 6.19 | 1.19 | 8.83 | 0.310 | 10.1 | 29.9 |
| MEG 50 | 6.23 | 1.23 | 8.94 | 0.312 | 10.5 | 32.3 |

[a] Base case.

used (i.e., the heat transfer rate decreased by approximately 6% for MEG 25). Only the use of higher concentrations of antifreeze caused considerable decreases in the heat transfer rates (i.e., a decrease of approximately 11% for MEG 50), but these percentages are hardly needed in practical situations. No remarkable variations of the vertical stress (and related strain and displacement) distributions in the foundation were observed with the variation of the heat carrier fluid compositions.

- In all of the cases, the decay of the thermal power extracted from the ground that was gained by the operative fluid occurred in the first 5 days of continuous functioning. In this period, the heat transfer rate decreased up to 30% with respect to the first day of operation for the energy pile equipped with a single U-shaped pipe and up to 45% for the foundation characterised by the double U and W-shaped pipe configurations.
- The choice of the most appropriate design solution for the heat exchange operation of the energy piles should be considered based on the energy demand of the related environment with respect to the thermo-hydraulic requirements of the heat pumps and in consideration of the magnitude of the involved effects from the geotechnical point of view.

## References


[1] H. Carslaw, J. Jaeger, Conduction of Heat in Solids, Oxford University Press, Oxford, United Kingdom, 1986.
[2] L. Ingersoll, H. Plass, Theory of the ground pipe heat source for the heat pump, ASHVE Trans. 47 (7) (1948) 339–348.
[3] J. Claesson, P. Eskilson, Conductive heat extraction to a deep borehole: thermal analyses and dimensioning rules, Energy 13 (6) (1988) 509–527.
[4] H. Zeng, N. Diao, Z. Fang, A finite line-source model for boreholes in geothermal heat exchangers, Heat Transf.-Asian Res. 31 (7) (2002) 558–567.
[5] L.R. Ingersoll, O.J. Zabel, A.C. Ingersoll, Heat Conduction with Engineering, Geological, and Other Applications, Mc-Graw Hill, New York, United States, 1954.
[6] L. Lamarche, B. Beauchamp, A new contribution to the finite line-source model for geothermal boreholes, Energy Build. 39 (2) (2007) 188–198.
[7] J. Bennet, J. Claesson, G. Hellstrom, Multipole Method to Compute the Conductive Heat Flows to and between Pipes in a Composite Cylinder, University of Lund, Lund, Sweden, 1987.
[8] T.V. Bandos, Á. Montero, E. Fernández, J.L.G. Santander, J.M. Isidro, J. Pérez, et al., Finite line-source model for borehole heat exchangers: effect of vertical temperature variations, Geothermics 38 (2) (2009) 263–270.
[9] X. Moch, M. Palomares, F. Claudon, B. Souyri, B. Stutz, Geothermal helical heat exchangers: comparison and use of two-dimensional axisymmetric models, Appl. Therm. Eng. 73 (1) (2014) 691–698.
[10] S. Erol, B. François, Efficiency of various grouting materials for borehole heat exchangers, Appl. Therm. Eng. 70 (1) (2014) 788–799.
[11] K. Kupiec, B. Larwa, M. Gwadera, Heat transfer in horizontal ground heat exchangers, Appl. Therm. Eng. 75 (2015) 270–276, http://dx.doi.org/10.1016/j.applthermaleng.2014.10.003.
[12] P. Eskilson, J. Claesson, Simulation model for thermally interacting heat extraction boreholes, Numer. Heat. Transf. 13 (2) (1988) 149–165.
[13] G. Hellström, Ground Heat Storage: Thermal Analyses of Duct Storage Systems, Lund University, Lund, Sweden, 1991.
[14] C. Yavuzturk, J.D. Spitler, A short time step response factor model for vertical ground loop heat exchangers, ASHRAE Trans. 105 (2) (1999) 475–485.
[15] M.G. Sutton, R.J. Couvillion, D.W. Nutter, R.K. Davis, An algorithm for approximating the performance of vertical bore heat exchangers installed in a stratified geological regime, ASHRAE Trans. 108 (2) (2002) 177–184.
[16] L. Lamarche, B. Beauchamp, New solutions for the short-time analysis of geothermal vertical boreholes, Int. J. Heat Mass Transf. 50 (7) (2007) 1408–1419.
[17] C. Lee, H. Lam, Computer simulation of borehole ground heat exchangers for geothermal heat pump systems, Renew. Energy 33 (6) (2008) 1286–1296.
[18] D. Marcotte, P. Pasquier, The effect of borehole inclination on fluid and ground temperature for GLHE systems, Geothermics 38 (4) (2009) 392–398.
[19] D. Marcotte, P. Pasquier, Fast fluid and ground temperature computation for geothermal ground-loop heat exchanger systems, Geothermics 37 (6) (2008) 651–665.
[20] R. Al-Khoury, P. Bonnier, R. Brinkgreve, Efficient finite element formulation for geothermal heating systems. Part I: steady state, Int. J. Numer. Methods Eng. 63 (7) (2005) 988–1013.
[21] R. Al-Khoury, P. Bonnier, Efficient finite element formulation for geothermal heating systems. Part II: transient, Int. J. Numer. Methods Eng. 67 (5) (2006) 725–745.
[22] S. Signorelli, S. Bassetti, D. Pahud, T. Kohl, Numerical evaluation of thermal response tests, Geothermics 36 (2) (2007) 141–166.
[23] D. Marcotte, P. Pasquier, On the estimation of thermal resistance in borehole thermal conductivity test, Renew. Energy 33 (11) (2008) 2407–2415.
[24] L. Lamarche, S. Kajl, B. Beauchamp, A review of methods to evaluate borehole thermal resistances in geothermal heat-pump systems, Geothermics 39 (2) (2010) 187–200.
[25] J. Wang, E. Long, W. Qin, Numerical simulation of ground heat exchangers based on dynamic thermal boundary conditions in solid zone, Appl. Therm. Eng. 59 (1) (2013) 106–115.
[26] B. Bouhacina, R. Saim, H.F. Oztop, Numerical investigation of a novel tube design for the geothermal borehole heat exchanger, Appl. Therm. Eng. 79 (2015) 153–162, http://dx.doi.org/10.1016/j.applthermaleng.2015.01.027.
[27] Y.-P. Chen, Y.-J. Sheng, C. Dong, J.-F. Wu, Numerical simulation on flow field in circumferential overlap trisection helical baffle heat exchanger, Appl. Therm. Eng. 50 (1) (2013) 1035–1043.
[28] L. Pu, D. Qi, K. Li, H. Tan, Y. Li, Simulation study on the thermal performance of vertical U-tube heat exchangers for ground source heat pump system, Appl. Therm. Eng. 79 (2015) 202–213, http://dx.doi.org/10.1016/j.applthermaleng.2014.12.068.
[29] X. Moch, M. Palomares, F. Claudon, B. Souyri, B. Stutz, Geothermal helical heat exchangers: coupling with a reversible heat pump in western Europe, Appl. Therm. Eng. 81 (2015) 368–375, http://dx.doi.org/10.1016/j.applthermaleng.2015.01.072.
[30] A. Zarrella, A. Capozza, M. De Carli, Performance analysis of short helical borehole heat exchangers via integrated modelling of a borefield and a heat pump: a case study, Appl. Therm. Eng. 61 (2) (2013) 36–47.
[31] A. Balbay, M. Esen, Temperature distributions in pavement and bridge slabs heated by using vertical ground-source heat pump systems, Acta Sci. Technol. 35 (4) (2013) 677–685.
[32] S. Abdelaziz, C. Olgun, J. Martin, Design and operational considerations of geothermal energy piles, in: Geo-Frontiers: Advances in Geotechnical Engineering, ASCE, Dallas, Texas, United States, 2011, pp. 450–459.
[33] B.C. Kwag, M. Krarti, Performance of thermoactive foundations for commercial buildings, J. Sol. Energy Eng. 135 (4) (2013), http://dx.doi.org/10.1115/1.4025587.
[34] J. Gao, X. Zhang, J. Liu, K.S. Li, J. Yang, Thermal performance and ground temperature of vertical pile-foundation heat exchangers: a case study, Appl. Therm. Eng. 28 (17) (2008) 2295–2304.

[35] M. Krarti, J.S. McCartney, Analysis of thermo-active foundations with U-tube heat exchangers, J. Sol. Energy Eng. 134 (2) (2012), http://dx.doi.org/10.1115/1.4005755.
[36] D. Bozis, K. Papakostas, N. Kyriakis, On the evaluation of design parameters effects on the heat transfer efficiency of energy piles, Energy Build. 43 (4) (2011) 1020–1029.
[37] T. Ozudogru, C. Olgun, A. Senol, 3D numerical modeling of vertical geothermal heat exchangers, Geothermics 51 (1) (2014) 312–324.
[38] S.L. Abdelaziz, T.Y. Ozudogru, C.G. Olgun, J.R. Martin II, Multilayer finite line source model for vertical heat exchangers, Geothermics 51 (1) (2014) 406–416.
[39] S.L. Abdelaziz, C.G. Olgun, J.R. Martin II, Equivalent energy wave for long-term analysis of ground coupled heat exchangers, Geothermics 53 (1) (2015) 67–84.
[40] Y. Man, H. Yang, N. Diao, J. Liu, Z. Fang, A new model and analytical solutions for borehole and pile ground heat exchangers, Int. J. Heat Mass Transf. 53 (13) (2010) 2593–2601.
[41] D. Pahud, M. Hubbuch, Measured thermal performances of the energy pile system of the dock midfield at Zürich Airport, in: European Geothermal Congress, Bundesverband Geothermie, Unterhaching, Germany, 2007.
[42] D. Pahud, B. Matthey, Comparison of the thermal performance of double U-pipe borehole heat exchangers measured in situ, Energy Build. 33 (5) (2001) 503–507.
[43] F. Loveridge, T. Amis, W. Powrie, Energy pile performance and preventing ground freezing, in: International Conference on Geomechanics and Engineering, Woodhead Publishing, Seoul, South Korea, 2012.
[44] T. Brettmann, T. Amis, Thermal conductivity analysis of geothermal energy piles, in: Geotechnical Challenges in Urban Regeneration Conference, Deep Foundations Institute, ASCE, London, United Kingdom, 2011, pp. 499–508.
[45] W.H. Thompson III, Numerical Analysis of Thermal Behavior and Fluid Flow in Geothermal Energy Piles, Virginia Polytechnic Institute and State University, Blacksburg, United States, 2013.
[46] F. Loveridge, C.G. Olgun, T. Brettmann, W. Powrie, The thermal behaviour of three different auger pressure grouted piles used as heat exchangers, Geotech. Geol. Eng. (2014) 1–17.
[47] A. Zarrella, M. De Carli, A. Galgaro, Thermal performance of two types of energy foundation pile: helical pipe and triple U-tube, Appl. Therm. Eng. 61 (2) (2013) 301–310.
[48] T.Y. Ozudogru, O. Ghasemi-Fare, C.G. Olgun, P. Basu, Numerical modeling of vertical geothermal heat exchangers using finite difference and finite element techniques, Geotech. Geol. Eng. (2015) 1–16.
[49] R. Saggu, T. Chakraborty, Thermal analysis of energy piles in sand, Geomech. Geoengin. Int. J. 10 (1) (2015) 10–29.
[50] M. Suryatriyastuti, H. Mroueh, S. Burlon, Understanding the temperature-induced mechanical behaviour of energy pile foundations, Renew. Sustain. Energy Rev. 16 (5) (2012) 3344–3354.
[51] C. Knellwolf, H. Peron, L. Laloui, Geotechnical analysis of heat exchanger piles, J. Geotech. Geoenviron. Eng. 137 (10) (2011) 890–902.
[52] T. Mimouni, L. Laloui, Towards a secure basis for the design of geothermal piles, Acta Geotech. 9 (3) (2014) 355–366.
[53] L. Laloui, M. Nuth, L. Vulliet, Experimental and numerical investigations of the behaviour of a heat exchanger pile, Int. J. Numer. Anal. Methods Geomech. 30 (8) (2006) 763–781.
[54] C.G. Olgun, T.Y. Ozudogru, C. Arson, Thermo-mechanical radial expansion of heat exchanger piles and possible effects on contact pressures at pile–soil interface, Géotech. Lett. 4 (July–September 2014) 170–178.
[55] T.Y. Ozudogru, C.G. Olgun, C.F. Arson, Analysis of friction induced thermo-mechanical stresses on a heat exchanger pile in isothermal soil, Geotech. Geol. Eng. (2014) 1–15.
[56] R. Saggu, T. Chakraborty, Cyclic thermo-mechanical analysis of energy piles in sand, Geotech. Geol. Eng. (2014) 1–22.
[57] A. Di Donna, L. Laloui, Numerical analysis of the geotechnical behaviour of energy piles, Int. J. Numer. Anal. Methods Geomech. (2014), http://dx.doi.org/10.1002/nag.2341.
[58] A.F. Rotta Loria, A. Gunawan, C. Shi, L. Laloui, C.W.W. Ng, Numerical modelling of energy piles in saturated sand subjected to thermo-mechanical loads, Geomech. Energy Environ. 1 (1) (2015) 1–15, http://dx.doi.org/10.1016/j.gete.2015.03.002.
[59] A.F. Rotta Loria, A. Di Donna, L. Laloui, Numerical study on the suitability of centrifuge testing for capturing the thermal-induced mechanical behavior of energy piles, J. Geotech. Geoenviron. Eng. (2015), http://dx.doi.org/10.1061/(ASCE)GT.1943-5606.0001318.
[60] W. Wang, R. Regueiro, J. McCartney, Coupled axisymmetric thermo-poro-mechanical finite element analysis of energy foundation centrifuge experiments in partially saturated silt, Geotech. Geol. Eng. (2014) 1–16.
[61] C.G. Olgun, T.Y. Ozudogru, S.L. Abdelaziz, A. Senol, Long-term performance of heat exchanger piles, Acta Geotech. (2014), http://dx.doi.org/10.1007/s11440-014-0334-z.
[62] E.H.N. Gashti, M. Malaska, K. Kujala, Evaluation of thermo-mechanical behaviour of composite energy piles during heating/cooling operations, Eng. Struct. 75 (1) (2014) 363–373.
[63] C. Casarosa, P. Conti, A. Franco, W. Grassi, D. Testi, Analysis of thermodynamic losses in ground source heat pumps and their influence on overall system performance, J. Phys. Conf. Ser. 547 (012006) (2014) 1–10.
[64] P. Conti, W. Grassi, D. Testi, Proposal of a holistic design procedure for ground source heat pump systems, in: European Geothermal Congress. Pisa, Italy, 2013.
[65] P. Conti, D. Testi, Seasonal thermal performance of geothermal piles, in: European COMSOL Conference. Milan, Italy, 2012.
[66] A. Di Donna, A.F. Rotta Loria, L. Laloui, Numerical study on the response of a group of energy piles under different combinations of thermo-mechanical loads, Comput. Geotech. (2015) submitted for publication.
[67] T. Mimouni, L. Laloui, Full-scale in situ testing of energy piles, in: L. Laloui, A. Di Donna (Eds.), Energy Geostructures: Innovation in Underground Engineering, Wiley-ISTE, 2013, pp. 23–43.
[68] T. Mimouni, L. Laloui, Behaviour of a group of energy piles, Can. Geotech. J. (2015) submitted for publication.
[69] L. Laloui, M. Moreni, L. Vulliet, Behaviour of a bi-functional pile, foundation and heat exchanger (in French), Can. Geotech. J. 40 (2) (2003) 388–402.
[70] V. Gnielinski, New equations for heat and mass transfer in turbulent pipe and channel flow, Int. Chem. Eng. 16 (1) (1976) 359–368.
[71] S. Haaland, Simple and explicit formulas for the friction factor in turbulent flow, J. Fluids Eng. – Trans. ASME 103 (1) (1983) 89–90.
[72] COMSOL, COMSOL Multiphysics Version 4.4: User's Guide and Reference Manual, COMSOL, Burlington, Massachusetts, United States, 2014.
[73] S. Lazzari, A. Priarone, E. Zanchini, Long-term performance of BHE (borehole heat exchanger) fields with negligible groundwater movement, Energy 35 (12) (2010) 4966–4974.
[74] L. Laloui, M. Moreni, G. Steinmann, A. Fromentin, D. Pahud, Test in Real Conditions of the Static Behaviour of a Pile Subjected to Thermomechanical Solicitations (in French). Internal report, Swiss Federal Institute of Technology in Lausanne (EPFL), Lausanne, Switzerland, 1998.
[75] A.F. Rotta Loria, A. Di Donna, L. Laloui, From in-Situ Tests to Numerical Simulations: the Response of an Energy Pile Foundation, Internal report, Swiss Federal Institute of Technology in Lausanne (EPFL), Lausanne, Switzerland, 2013.
[76] A. Lavine, D. DeWitt, T. Bergman, F. Incropera, Fundamentals of Heat and Mass Transfer, Wiley, Hoboken, New Jersey, United States, 2011.